

Dynamic Spiking Framework for Graph Neural Networks

Nan Yin¹, Mengzhu Wang², Zhenghan Chen³, Giulia De Masi⁴, Huan Xiong^{5,1*}, Bin Gu^{6,1*}

¹Mohamed bin Zayed University of Artificial Intelligence

²School of Artificial Intelligence, Hebei University of Technology

³Microsoft Corporation

⁴Technology Innovation Institute

⁵Harbin Institute of Technology

⁶Jilin University

{yinnan8911,dreamkily,pandaarych,jsgubin,
huan.xiong.math}@gmail.com, giulia.demasi@tii.ae

Abstract

The integration of Spiking Neural Networks (SNNs) and Graph Neural Networks (GNNs) is gradually attracting attention due to the low power consumption and high efficiency in processing the non-Euclidean data represented by graphs. However, as a common problem, dynamic graph representation learning faces challenges such as high complexity and large memory overheads. Current work often uses SNNs instead of Recurrent Neural Networks (RNNs) by using binary features instead of continuous ones for efficient training, which would overlooks graph structure information and leads to the loss of details during propagation. Additionally, optimizing dynamic spiking models typically requires propagation of information across time steps, which increases memory requirements. To address these challenges, we present a framework named *Dynamic Spiking Graph Neural Networks* (Dy-SIGN). To mitigate the information loss problem, Dy-SIGN propagates early-layer information directly to the last layer for information compensation. To accommodate the memory requirements, we apply the implicit differentiation on the equilibrium state, which does not rely on the exact reverse of the forward computation. While traditional implicit differentiation methods are usually used for static situations, Dy-SIGN extends it to the dynamic graph setting. Extensive experiments on three large-scale real-world dynamic graph datasets validate the effectiveness of Dy-SIGN on dynamic node classification tasks with lower computational costs.

Introduction

Graph Neural Networks (GNNs) (Scarselli et al. 2008) have been widely applied in various fields to learn the graph representation by capturing the dependencies of nodes and edges, such as relation detection (Schlichtkrull et al. 2018; Chen, Li, and Tang 2020; Mi and Chen 2020; Xu et al. 2019b; Ju et al. 2024) and recommendation (Wu et al. 2022). However, most GNNs are primarily designed for static or non-temporal graphs, which cannot meet the requirement of dynamic evolution over time in practice. The established solution is to extend the dynamic graphs into sequence models directly. Typically, these methods (Yin et al. 2023b; Shi

et al. 2021; Kumar, Zhang, and Leskovec 2019; Yin et al. 2022a) utilize the Recurrent Neural Networks (RNNs) (Cho et al. 2014) to capture the dynamic evolution of graphs for numerous downstream tasks such as time series prediction or graph property prediction (Yin et al. 2022b; Wieder et al. 2020; Yin et al. 2023a, 2024b; Pang et al. 2023).

Despite the promising performance of dynamic graphs, the majority of these approaches typically involve complex structures that consume significant computational resources during training and testing. Inspired by the way the brain process information, Spiking Neural Networks (SNNs) represent the event or clock-driven signals as inference for updating the neuron nodes parameters (Brette et al. 2007). Different from traditional deep learning methods, SNNs utilize discrete spikes information instead of continuous features, resulting in significantly lower power consumption during model training. Considering the inherent characteristics of SNNs (Maass 1997; Pfeiffer and Pfeil 2018; Schliebs and Kasabov 2013), a few recent works (Zhu et al. 2022; Xu et al. 2021; Li et al. 2023; Yin et al. 2024a) have attempted to integrate SNNs into the GNNs framework to tackle the issue of high computational complexity. These methods transform the node features into a series of spikes with Poisson rate coding, and follow a graph convolution layer with SNN neurons, which employ a membrane potential threshold to convert continuous features to spike information (Kim et al. 2020; Bu et al. 2022). Although Spiking Graph Networks (SGNs) are gradually gaining attention, the use of SNNs in dynamic graphs is still less explored, which is a more common scenario in life. To address the gap, the work focuses on the problem of *spiking dynamic graph*, which applies SNNs for dynamic graph node classification.

However, the problem is highly challenging due to the following reasons: (1) *Information Loss*. The representation of GNNs includes the information on graph structure and neighboring nodes, which are crucial for downstream tasks. However, SNNs employ spike signals instead of continuous features, leading to the loss of details regarding the structure and neighbors. Moreover, with the evolution of graphs over time, the information loss issue may further deteriorate the graph representation. (2) *Memory Consumption*. The RNN-based dynamic graph methods typically require signif-

*Corresponding authors.

icant memory resources to store the temporal node information (Sak, Senior, and Beaufays 2014). Moreover, SNNs inherently operate with multiple time latencies (i.e., calculate the spike signals with time latency steps in each SNN layer). If we simply replace the GNN layer with the SNN layer on each time step, we need to store the temporary spikes in SNN layer and temporal information at each time step simultaneously, which further exacerbates memory consumption.

In this paper, we present a novel framework named Dynamic Spiking Graph Neural Networks (Dy-SIGN) for node classification. The primary insight of proposed Dy-SIGN is to thoroughly explore how to apply SNNs to dynamic graphs, and address the challenges of information loss and memory consumption by using the information compensation mechanism and implicit differentiation on the equilibrium state. On the one hand, the information compensation mechanism aims to make up for the information loss during forward propagation. However, implementing the mechanism in each layer of SNNs would significantly increase the model complexity. Thus, we propose to establish an information channel between the shallow and final layers to incorporate the original information directly into feature representations. This approach not only reduces the model complexity but also mitigates the impact of information loss. On the other hand, inspired by recent advances in implicit methods (Bai, Koltun, and Kolter 2020; Xiao et al. 2021) that view neural networks as solving an equilibrium equation for fixed points and provide alternative implicit models defined by the equation, we provide a variation training method that is suitable for dynamic spiking graph neural networks. Specifically, Dy-SIGN simplifies the non-differentiable items in backpropagation, thus avoiding the huge computational overhead of traditional SNNs due to the use of surrogate learning techniques. In this way, the calculation of the gradient would significantly reduce memory consumption. We conduct extensive experiments to demonstrate the effectiveness of proposed Dy-SIGN in comparison to the state-of-the-art methods across various scenarios.

In summary, our contributions are as follows: (1) *Motivation*: From the perspective of practical application and data analysis, we propose the Dy-SIGN, which is the first attempt to introduce implicit differentiation into dynamic graph. (2) *Methodology*: We propose a novel approach called Dy-SIGN that incorporates SNNs into dynamic graphs to release the information loss and memory consumption problem. (3) *Experiments*: Extensive experiments validate the superiority of the proposed Dy-SIGN over the state-of-the-art methods.

Related Work

SNN Training Methods

In the supervised training of SNNs, there are two primary research directions. One direction focuses on establishing a connection between the spike representations of SNNs, such as firing rates, and equivalent Artificial Neural Networks (ANNs) activation mappings. This connection enables the ANN-to-SNN conversion (Diehl et al. 2015; Hunsberger and Eliasmith 2015; Rueckauer et al. 2017; Rathi et al. 2020), and the optimization of SNNs using gradients computed

from this equivalent mappings (Thiele, Bichler, and Dupret 2020; Wu et al. 2021; Zhou et al. 2021; Xiao et al. 2021; Meng et al. 2022). These methods usually require a relatively large number of time-steps to achieve performance comparable to ANNs, suffering from high latency and usually more energy consumption. The other direction is to directly train SNNs with back-propagation (Bohte, Kok, and La Poutre 2000; Esser et al. 2015; Bellec et al. 2018; Huh and Sejnowski 2018), which typically employs the surrogate gradients (Shrestha and Orchard 2018) method to overcome the non-differentiable nature of the binary spiking functions and direct train SNNs from scratch. This follows the back-propagation through time (BPTT) framework. BPTT with surrogate gradients can achieve extremely low latency, however, it requires large training memory to maintain the computational graph unfolded over time.

Dynamic GNNs

Dynamic GNNs have achieved impressive performance in various tasks. With the help of RNNs (Cho et al. 2014), static GNNs can be extended to model dynamic processes by employing RNN architectures (Rossi et al. 2020; Pareja et al. 2020; Shi et al. 2021; Rossi et al. 2020; Xu et al. 2019a). TGN (Rossi et al. 2020) and JODIE (Kumar, Zhang, and Leskovec 2019) update the node hidden state by RNN units for representation learning. EvolveGCN (Pareja et al. 2020) uses the RNN to regulate the model parameters on each time step. However, the RNN-based dynamic graph methods could save the historical information for graph representation, they typically require massive computational costs and memory consumption. To effectively model the dynamic evolution of graphs while minimizing computational and memory requirements, we introduce the implicit models and SNNs into dynamic GNNs.

Feedback Models

Implicit models are promising approaches to deep learning that utilize implicit layers to determine the outputs. In contrast to explicit models, which typically require storing intermediate activations for backpropagation, implicit models use the fixed-point solution (Bai, Kolter, and Koltun 2019; Bai, Koltun, and Kolter 2020) to perform backpropagation without saving these intermediate activations. This results in constant complexity for the implicit models, which is a significant advantage for large models. DEQ (Bai, Kolter, and Koltun 2019) demonstrates the ability of implicit models in sequence modeling. MDEQ (Bai, Koltun, and Kolter 2020) incorporates multiscale modeling into implicit deep networks, enabling tasks such as image classification and semantic segmentation. To further enhance the efficiency of implicit models, (Gu et al. 2020) extend the concept of implicit fixed-point equilibrium to graph learning, to address the problem of evaluation and training for recurrent GNNs. (Liu et al. 2022) propose a multiscale graph neural network with implicit layers to model multiscale information on graphs at multiple resolutions. Although implicit models have shown promise in various areas, their application to dynamic spiking graphs is still relatively unexplored.

Preliminary

Spiking Neuron Models

SNNs utilize binary activations in each layer, which limits the representation capacity. To address the issue, SNNs introduce a temporal dimension, known as latency K . In the forward pass of SNNs, inputs are presented as streams of events and repeated for K time steps to produce the final result. The leaky-integrate-and-fire (LIF) model is commonly used to describe the dynamics of spiking neurons. In LIF, each neuron integrates the received spikes as the membrane potential $u_{\tau,i}$, which can be formulated as a first-order differential equation,

$$\text{LIF: } \bar{\lambda} \frac{du_{\tau}}{d\tau} = -(u_{\tau} - u_{rest})R \cdot I(\tau), \quad u_{\tau} < V_{th}, \quad (1)$$

where $I(\tau)$ is the input current, V_{th} is the spiking threshold, and R and $\bar{\lambda}$ are resistance and time constant, respectively. When u_{τ} reaches V_{th} at time τ , a spike is generated and u_{τ} is reset to the resting potential $u_{\tau} = u_{rest}$, which is usually taken as 0. The spike train is expressed by the Dirac delta function: $s_{\tau} = \sum_{t^f} \delta(\tau - t^f)$. We consider a simple current model $I_{\tau,i} = \sum_j w_{ij} s_{\tau,j} + b$, where w_{ij} is the weight from neuron j to neuron i . Then, the general form of LIF is described as:

$$\begin{cases} u_{\tau+1,i} = \lambda(u_{\tau,i} - V_{th}s_{\tau,i}) + \sum_j w_{ij}s_{\tau,j} + b, \\ s_{\tau+1,i} = \mathbb{H}(u_{\tau+1,i} - V_{th}), \end{cases} \quad (2)$$

where $\mathbb{H}(x)$ is the Heaviside step function, which is the non-differentiable spiking function. $s_{\tau,i}$ is the binary spike train of neuron i , and $\lambda < 1$ is a leaky term related to the constant τ_m and discretization time interval used in the LIF model. The constant R , $\bar{\lambda}$, and time step-size are absorbed into the weights w_{ij} and bias b . The training of SNNs follows the process of BPTT, and the gradients with K time latency steps are calculated with:

$$\begin{aligned} \frac{\partial \mathcal{L}}{\partial \mathbf{W}^l} &= \sum_{\tau=1}^K \frac{\partial \mathcal{L}}{\partial \mathbf{s}^{\tau,l+1}} \frac{\partial \mathbf{s}^{\tau,l+1}}{\partial \mathbf{u}^{\tau,l+1}} \left(\frac{\partial \mathbf{u}^{\tau,l+1}}{\partial \mathbf{W}^l} \right. \\ &+ \sum_{k < \tau} \prod_{i=\tau-1}^k \left(\frac{\partial \mathbf{u}_{i+1}^{l+1}}{\partial \mathbf{u}_i^{l+1}} + \frac{\partial \mathbf{u}_{i+1}^{l+1}}{\partial \mathbf{s}_i^{l+1}} \frac{\partial \mathbf{s}_i^{l+1}}{\partial \mathbf{u}_i^{l+1}} \right) \frac{\partial \mathbf{u}_k^{l+1}}{\partial \mathbf{W}^l} \Big), \end{aligned} \quad (3)$$

where \mathbf{W}^l is the trainable matrix on l -th layer and \mathcal{L} is the loss. The terms $\frac{\partial \mathbf{s}_{\tau}^l}{\partial \mathbf{u}_{\tau}^l}$ are non-differentiable, and surrogate derivatives are typically used instead.

Dynamic GNNs

Given the dynamic graph $\mathcal{G} = \{G_1, \dots, G_t, \dots, G_T\}$ with T time steps. On each snapshot $G_t = (\mathbf{A}_t, \mathbf{X}_t, \mathcal{V}_t, \mathcal{E}_t)$, where \mathbf{A}_t is the adjacency matrix, $\mathbf{X}_t \in \mathbb{R}^{N \times d}$ is N node features with dimension d , $\mathcal{V}_t = \{v_1^t, \dots, v_N^t\}$ and \mathcal{E}_t are the set of nodes and edges on time step t . Dynamic graph methods typically extract the graph features on each time step and then model the evolution over time, which is formulated as:

$$\begin{aligned} \mathbf{h}_v^{t,l} &= \mathcal{C}^{t,l}(\mathbf{h}_v^{t,l-1}, \mathcal{A}^{t,l}(\{\mathbf{h}_u^{t,l-1}\}_{u \in \mathcal{N}(v)})), \\ \mathbf{h}_v^{t+1} &= \text{Evo}(\mathbf{h}_v^{1,L}, \dots, \mathbf{h}_v^{t,L}), \end{aligned} \quad (4)$$

where $\mathcal{N}(v)$ is the neighbors of v . $\mathcal{A}^{t,l}$ and $\mathcal{C}^{t,l}$ denote the aggregation and combination operations at the l -th layer on time step t , respectively. L is the number of layers of a graph and Evo means the evolution operation over time 1 to t , which is typically implemented with RNN (Cho et al. 2014) or LSTM (Hochreiter and Schmidhuber 1997).

The Proposed Dy-SIGN

Overview

This paper introduces a novel approach named Dy-SIGN for semi-supervised dynamic spiking graph node classification. Recognizing that if the time latency τ in SNN tends to infinity, models will retain the details information of input. However, since the large τ would cause the vanishing gradient problem (Hochreiter 1998) and significantly increase the complexity, we propose the information compensation mechanism that bridges the feature from the beginning to the last layer and includes the shallow representation in the final embedding. Additionally, we propose a variation of the training method in dynamic graph, which is proved to be equivalent to the implicit differentiation. This method simplifies the calculation of gradient, which relies on the equation of implicit differentiation rather than the forward procedure, thereby reducing memory consumption. The detailed illustration of our Dy-SIGN can be seen in Figure 1, and we will introduce Dy-SIGN in detail.

Information Compensation Spiking Graph Neural Network

Spiking Graph Network (SGN) (Zhu et al. 2022; Xu et al. 2021) usually applies the Bernoulli encoding to transform the node representation to the spike signals for propagation. Specifically, on time step $t \in [1, \dots, T]$ with T denotes the length of dynamic graph time window, we have the graph $G_t = (\mathbf{A}_t, \mathbf{X}_t)$, where \mathbf{A}_t is the adjacency matrix of G_t and \mathbf{X}_t is the node features. SGN first encodes the initial features into binary signals $\{\tilde{\mathbf{X}}_{t,1}, \dots, \tilde{\mathbf{X}}_{t,\tau}, \dots, \tilde{\mathbf{X}}_{t,K}\}$, where $\tau \in [1, \dots, K]$ means the time latency step in SGN, and K is the length of SGN time latency window. Then, the **layer-wise** (update on different layers) spiking graph propagation is defined as:

$$\mathbf{s}_{t,\tau}^l = \Phi(\text{Cov}(\mathbf{A}, \mathbf{s}_{t,\tau}^{l-1}), \mathbf{s}_{t,\tau-1}^l), \quad (5)$$

where Cov is the graph convolutional layer which is the same as Equation 4, $\mathbf{s}_{t,\tau}^l$ denotes the nodes spiking features on time step t and time latency step τ with l -th layer. $\mathbf{S}_{t,1}^l = \tilde{\mathbf{X}}_{t,1}$, $\Phi(\cdot)$ is the non-linear function that combine historical information $\mathbf{S}_{t,\tau-1}^l$ into current state. After that, the **temporal-wise** (update on each time latency in SGN) membrane potentials and firing rate follows:

$$\begin{cases} \mathbf{u}_{t,\tau+1}^l = \lambda \mathbf{u}_{t,\tau}^l (1 - \mathbf{s}_{t,\tau}^l) + \sum \mathbf{W}^l \text{Con}(\mathbf{A}, \mathbf{s}_{t,\tau+1}^{l-1}), \\ \mathbf{s}_{t,\tau+1}^l = \mathbb{H}(\mathbf{u}_{t,\tau+1}^l - V_{th}). \end{cases}$$

For the specific node representation $\mathbf{x}_i = [\mathbf{x}_{i1}, \dots, \mathbf{x}_{id}]$, where \mathbf{x}_i denotes the i -th node features of graph, and d is the feature dimension. The spiking signals are sampled with Bernoulli distribution with K time latency in SGN, which

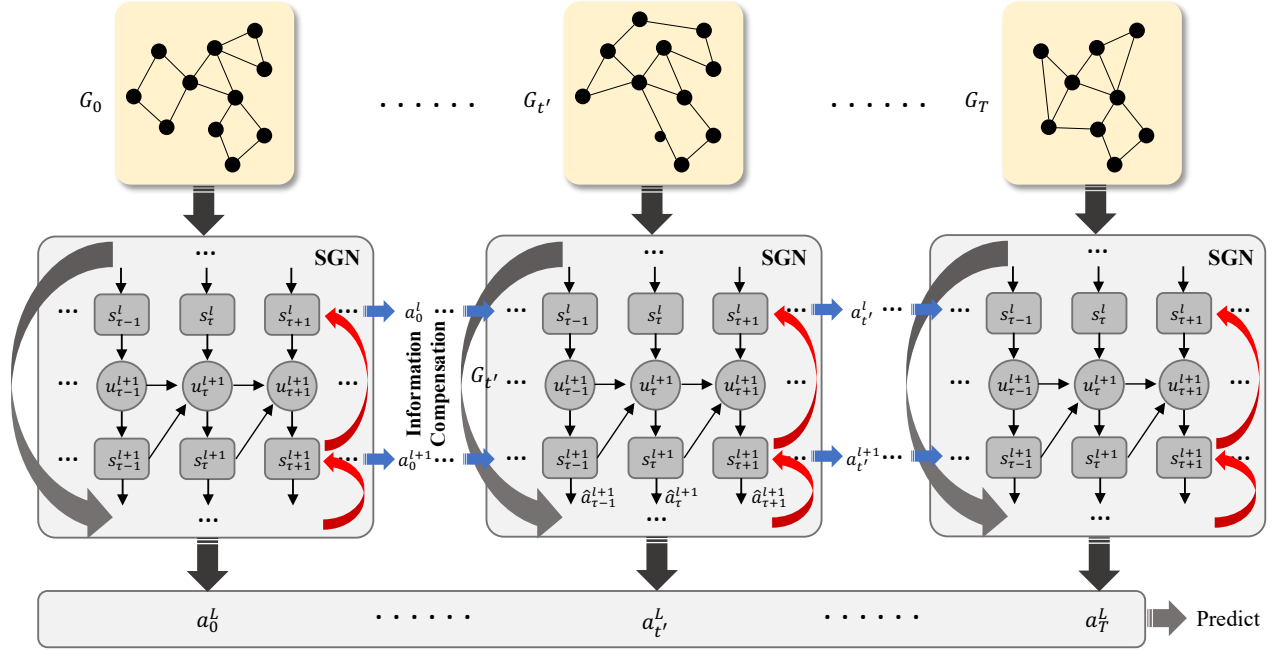


Figure 1: An overview of the proposed Dy-SIGN. The Spiking Graph Neural Network (SGN) combines the SNNs and GNNs for node representation learning. The information compensation mechanism transfers the information from the shallow layer to the last to mitigate the information loss issue. The variation training method is applied to calculate the fix-point on each time latency in SGN and is used for dynamic prediction.

is denoted as $\tilde{\mathbf{x}}_i = \{\tilde{\mathbf{x}}_{1,i}, \dots, \tilde{\mathbf{x}}_{\tau,i}, \dots, \tilde{\mathbf{x}}_{K,i}\}$ with $\tilde{\mathbf{x}}_{\tau,i} = [\tilde{\mathbf{x}}_{\tau,i1}, \dots, \tilde{\mathbf{x}}_{\tau,id}]$. Then we have $P(\tilde{\mathbf{x}}_{\tau,ij} = 1) = \mathbf{x}_{ij}$ and $P(\tilde{\mathbf{x}}_{\tau,ij} = 0) = 1 - \mathbf{x}_{ij}$. Assume the parameters of each spike neuron are $w_i = [w_{i1}, \dots, w_{id}]$, the combined spike input z_i for the next SGN layer holds:

$$z_{\tau,i} = \sum_{j=1}^d w_{ij} \tilde{\mathbf{x}}_{\tau,ij}^{\tau}, \quad (6)$$

$$\mathbb{E}(z_{\tau,i}) = \sum_{j=1}^d w_{ij} \mathbb{E}(\tilde{\mathbf{x}}_{\tau,ij}^{\tau}) = \sum_{j=1}^d w_{ij} \mathbf{x}_{ij}.$$

According to (Chung and Lu 2002), the error bound of SGN holds:

$$\lim_{\tau \rightarrow \infty} P(z_{\tau,i} < \mathbb{E}(z_{\tau,i}) - \epsilon) \leq e^{-\epsilon^2/2\sigma},$$

$$\lim_{\tau \rightarrow \infty} P(z_{\tau,i} > \mathbb{E}(z_{\tau,i}) + \epsilon) \leq e^{-\epsilon^2/2(\sigma + \hat{w}_i \epsilon/3)}, \quad (7)$$

where $\hat{w}_i = \max\{w_{i1}, \dots, w_{id}\}$. From Equation 7, we observe that as $\tau \rightarrow \infty$, the difference between SGN and GNN will be with the probability of $p = e^{-\epsilon^2/2(\sigma + \hat{w}_i \epsilon/3)}$ to exceed the upper and lower bounds. This reveals that the spiking signals would preserve the details information of continuous features when $\tau \rightarrow \infty$. However, with the increase of τ , SGN becomes difficult to train and may suffer from the vanishing gradient problem due to the coefficient of λ in Equation 6. To address the issue, we design the information compensation mechanism for SGN that directly transfers features from the first layer to the last layer for node

embeddings. Formally:

$$\begin{cases} \mathbf{u}_{\tau}^1 = \lambda \mathbf{u}_{\tau}^1 - 1 + \mathbf{W}^1 \mathbf{s}_{\tau}^N + \mathbf{F}^1 \mathbf{x}_{\tau} - V_{th} \mathbf{s}_{\tau}^1, \\ \mathbf{u}_{\tau}^l = \lambda \mathbf{u}_{\tau-1}^l + \mathbf{F}^l \mathbf{s}_{\tau}^{l-1} - V_{th} \mathbf{s}_{\tau}^l, \quad l = 2, \dots, N, \end{cases}$$

where \mathbf{u}_{τ}^l denotes the neuronal membrane potential at time τ on l -th layer. \mathbf{F}^l and \mathbf{W}^l are the trainable parameters on the l -th layer, \mathbf{F}^1 is the information compensation matrix. In this way, the information compensation SGN follows the form of multi-layer structures of feedback model (Bai, Kolter, and Koltun 2019; Bai, Koltun, and Kolter 2020). This type of structure has several potential advantages: (1) The forward and backward procedures are decoupled, avoiding the problem of non-differentiable spiking functions. (2) Using implicit differentiation in the equilibrium state, we can compute the gradient without saving the exact forward procedure, thus reducing memory consumption.

Variation of Training SGN

The traditional training method of SGN follows BPTT, which replaces the non-differentiable term $\frac{\partial \mathbf{s}_{\tau}^l}{\partial \mathbf{u}_{\tau}^l}$ with the surrogate derivatives in Equation 3. However, BPTT relies on multiple backpropagation paths, which would consume a large amount of memory. Similarly to (Xiao et al. 2022), we set the gradient of the Heaviside step function to 0, which is formulated as $\frac{\partial \mathbf{u}_{\tau+1}^l}{\partial \mathbf{s}_{\tau+1}^{l+1}} \frac{\partial \mathbf{s}_{\tau}^{l+1}}{\partial \mathbf{u}_{\tau}^{l+1}} = 0$. Then, the gradient of pa-

parameters \mathbf{W}^l is:

$$\begin{aligned} \frac{\partial L}{\partial \mathbf{W}^l} &= \sum_{\tau=1}^K \frac{\partial L}{\partial \mathbf{s}_{\tau}^{l+1}} \frac{\partial \mathbf{s}_{\tau}^{l+1}}{\partial \mathbf{u}_{\tau}^{l+1}} \left(\sum_{k \leq \tau} \lambda^{\tau-k} \frac{\partial \mathbf{u}_k^{l+1}}{\partial \mathbf{W}^l} \right) \\ &= \sum_{\tau=1}^K \frac{\partial L}{\partial \mathbf{s}_{\tau}^{l+1}} \frac{\partial \mathbf{s}_{\tau}^{l+1}}{\partial \mathbf{u}_{\tau}^{l+1}} \left(\sum_{k \leq \tau} \lambda^{\tau-k} \mathbf{s}_k^l \right). \end{aligned} \quad (8)$$

During the forward procedure is $\hat{\mathbf{a}}_{\tau+1}^l = \lambda \hat{\mathbf{a}}_{\tau}^l + \mathbf{s}_{\tau+1}^l$, where the presynaptic activities can be denoted as $\hat{\mathbf{a}}_{\tau+1}^l = \sum_{k \leq \tau} \lambda^{\tau-k} \mathbf{s}_k^l$. By calculating the gradient of $\frac{\partial L}{\partial \mathbf{s}_{\tau}^{l+1}} \frac{\partial \mathbf{s}_{\tau}^{l+1}}{\partial \mathbf{u}_{\tau}^{l+1}}$, we can directly compute the value of Equation 8 without considering the backpropagation through $\frac{\partial \mathbf{u}_{\tau+1}^{l+1}}{\partial \mathbf{u}_{\tau}^{l+1}}$, which would decrease the complexity and memory consumption of the model. On each time latency τ , the output is denoted as $\hat{\mathbf{a}}_{\tau}^{l+1}$, and the output of the SGN is $\{\hat{\mathbf{a}}_1^l, \dots, \hat{\mathbf{a}}_{\tau}^l, \dots, \hat{\mathbf{a}}_K^l\}$ on l -th layer.

Comparing with Feedback Model

Note that, in the spiking dynamic graph framework, $t \in [1, \dots, T]$ stands for the time steps of each graph, and $\tau \in [1, \dots, K]$ is the time latency in SGN. At each time step t , we apply the information compensation SGN to extract the graph features as Equation 8. In the traditional feedback model, the weighted average firing rate and inputs are denoted as $\mathbf{a}_{t,K} = \frac{\sum_{\tau=1}^K \lambda^{K-\tau} \mathbf{s}_{t,\tau}}{\sum_{\tau=1}^K \lambda^{K-\tau}}$ and $\bar{\mathbf{x}}_{t,K} = \frac{\sum_{\tau=0}^K \lambda^{K-\tau} \mathbf{x}_{t,\tau}}{\sum_{\tau=0}^K \lambda^{K-\tau}}$, where $\mathbf{s}_{t,\tau}$ and $\mathbf{x}_{t,\tau}$ denote the firing rate and input on time latency τ in SGN and on time step t of dynamic graph. The LIF model approximate an equilibrium point \mathbf{a}_t^* that satisfies $\mathbf{a}_t^* = \sigma \left(\frac{1}{V_{th}} (\mathbf{W} \mathbf{a}_t^* + \mathbf{F} \mathbf{x}_t^*) \right)$. The characteristic is similar to the presynaptic activities $\hat{\mathbf{a}}_{t,\tau+1}^l = \sum_{k \leq \tau} \lambda^{\tau-k} \mathbf{s}_{t,k}^l$. Considering the last time latency K on layer l , we have $\hat{\mathbf{a}}_{t,K}^l = \sum_{\tau=1}^K \lambda^{K-\tau} \mathbf{s}_{t,\tau}^l$, which equals to $C \mathbf{a}_{t,K}^l$ with $C = \sum_{\tau=1}^K \lambda^{K-\tau}$. In other words, the fire rate $\hat{\mathbf{a}}$ in at the last time latency step K on layer l is equivalent to the traditional feedback model. Thus, we prove that the variation of training SGN is equivalent to the traditional feedback model, and we can calculate the gradient of parameters with Equation 8 directly.

Dynamic Spiking Graph Neural Network

The proposed information compensation SGN is designed for a fixed time step t . However, since the graphs may change over time, it remains a challenge to integrate the temporal dynamics of SGN with dynamic graphs. We propose a novel method by propagating the medium $\mathbf{a}_{t,K} = \{\mathbf{a}_{t,K}^1, \dots, \mathbf{a}_{t,K}^l, \dots, \mathbf{a}_{t,K}^L\}$ at different time steps. At time step $t+1$, we set the initial membrane potential to $\mathbf{u}_{t+1,1} = \mathbf{a}_{t,K}$, and the update process of membrane potentials is:

$$\begin{aligned} \mathbf{u}_{t+1,K} &= \lambda \mathbf{u}_{t+1,K-1} + \mathbf{W} \mathbf{s}_{t+1,K-1} \\ &\quad + \mathbf{F} \mathbf{x}_{t+1,K-1} - V_{th} \mathbf{s}_{t+1,K}. \end{aligned} \quad (9)$$

Algorithm 1: Learning Algorithm of Dy-SIGN

Input: Dynamic graph $\mathcal{G} = \{G_1, \dots, G_T\}$; Label \mathbf{y} ; Network parameters θ ; Network layers L ; Time latency of SGN K .

Output: Trained model parameters θ .

- 1: Initialize θ .
 - 2: // **Forward:**
 - 3: **for** $t = 1, \dots, T$ **do**
 - 4: **for** $l = 1, \dots, L$ **do**
 - 5: Calculate the average firing rate $\mathbf{a}_{t,K}^l$ with Equation 10;
 - 6: Collect the fixed point representation \mathbf{a}_t^* on layer L and time step t ;
 - 7: **end for**
 - 8: **end for**
 - 9: Calculate the output of Dy-SIGN $\hat{\mathbf{y}}$ and the loss \mathcal{L} with Equation 11;
 - 10: // **Backward:**
 - 11: **for** $l = L, \dots, 1$ **do**
 - 12: Calculate the gradient of SGN with Equation 8;
 - 13: Update the parameters θ .
 - 14: **end for**
-

The average firing rates is defined as $\mathbf{a}_{t+1,K} = \frac{\sum_{\tau=1}^K \lambda^{K-\tau} \mathbf{s}_{t+1,\tau}}{\sum_{\tau=1}^K \lambda^{K-\tau}}$, the average inputs as $\bar{\mathbf{x}}_{t+1,K} = \frac{\sum_{\tau=0}^K \lambda^{K-\tau} \mathbf{x}_{t+1,\tau}}{\sum_{\tau=0}^K \lambda^{K-\tau}}$, and $\mathbf{u}_{t+1,1} = \mathbf{a}_{t,K}$, $\mathbf{s}_{t+1,1} = \mathbf{0}$. Then, we have:

$$\begin{aligned} \mathbf{a}_{t+1,K} &= \frac{1}{V_{th}} \left(\frac{\sum_{i=0}^{K-2} \lambda^i}{\sum_{i=0}^{K-1} \lambda^i} \mathbf{W} \mathbf{a}_{t+1,K-1} + \mathbf{F} \bar{\mathbf{x}}_{t+1,K-1} \right. \\ &\quad \left. - \frac{\mathbf{u}_{t+1,K}}{\sum_{i=0}^{K-1} \lambda^i} + \frac{\mathbf{a}_{t,K}}{\sum_{i=0}^{K-1} \lambda^i} \right) \\ &= \sigma \left(\frac{1}{V_{th}} \left(\frac{\sum_{i=0}^{K-2} \lambda^i}{\sum_{i=0}^{K-1} \lambda^i} \mathbf{W} \mathbf{a}_{t+1,K-1} \right. \right. \\ &\quad \left. \left. + \mathbf{F} \bar{\mathbf{x}}_{t+1,K-1} \right) \right) - \frac{\mathbf{u}_{t+1,K}}{V_{th} \sum_{i=0}^{K-1} \lambda^i} \\ &\quad + \frac{\mathbf{a}_{t,K}}{V_{th} \sum_{i=0}^{K-1} \lambda^i}, \end{aligned} \quad (10)$$

where $\sigma(x) = \begin{cases} 1, & x > 1 \\ x, & 0 \leq x \leq 1. \\ 0, & x < 0 \end{cases}$. For each time step t , we

will first calculate the equilibrium point $\mathbf{a}_{t,K} \rightarrow \mathbf{a}_t^*$, which is fixed for time step $t+1$. Therefore, the LIF model gradually approximates the equilibrium point \mathbf{a}_t^* that satisfies $\mathbf{a}_t^* = \sigma \left(\frac{1}{V_{th}} (\mathbf{W} \mathbf{a}_t^* + \mathbf{F} \mathbf{x}_t^*) \right)$ with $\bar{\mathbf{x}}_{t,K} \rightarrow \mathbf{x}_t^*$.

Finally, we have fixed point representation over time, i.e., $\mathbf{a}^* = \{\mathbf{a}_1^*, \dots, \mathbf{a}_t^*, \dots, \mathbf{a}_T^*\}$. We concatenate all the embeddings for the final node classification, which is formu-

| Methods | DBLP | | | Tmall | | | Patent | | |
|--------------------|------------------|------------------|------------------|------------------|------------------|------------------|------------------|------------------|------------------|
| | 40% | 60% | 80% | 40% | 60% | 80% | 40% | 60% | 80% |
| DeepWalk | 67.08 | 67.17 | 67.12 | 49.09 | 49.29 | 49.53 | 72.32±0.9 | 72.25±1.2 | 72.05±1.1 |
| Node2Vec | 66.07 | 66.81 | 66.93 | 54.37 | 54.55 | 54.58 | 69.01±0.9 | 69.08±0.9 | 68.99±1.0 |
| HTNE | 67.68 | 68.24 | 68.36 | 54.81 | 54.89 | 54.93 | - | - | - |
| M ² DNE | 69.02 | 69.48 | 69.75 | 57.75 | 57.99 | 58.47 | - | - | - |
| DyTriad | 60.45 | 64.77 | 66.42 | 44.98 | 48.97 | 51.16 | - | - | - |
| MPNN | 64.19±0.4 | 63.91±0.3 | 65.05±0.5 | 47.71±0.8 | 47.78±0.7 | 50.27±0.5 | - | - | - |
| JODIE | 66.73±1.0 | 67.32±1.1 | 67.53±1.3 | 52.62±0.8 | 54.02±0.6 | 54.17±0.2 | 77.57±0.8 | 77.69±0.6 | 77.67±0.4 |
| EvolveGCN | 67.22±0.3 | 69.78±0.8 | 71.20±0.7 | 53.02±0.7 | 54.99±0.7 | 55.78±0.6 | 79.67±0.4 | 79.76±0.5 | 80.13±0.4 |
| TGAT | 71.18±0.4 | 71.74±0.5 | 72.15±0.3 | 56.90±0.6 | 57.61±0.7 | 58.01±0.7 | 81.51±0.4 | 81.56±0.6 | 81.57±0.5 |
| SpikeNet | 70.88±0.4 | 71.98±0.3 | 74.64±0.5 | 58.84±0.4 | 61.13±0.8 | 62.40±0.6 | 83.53±0.6 | 83.85±0.7 | 83.90±0.6 |
| Dy-SIGN | 70.94±0.1 | 72.07±0.1 | 74.67±0.5 | 57.48±0.1 | 60.94±0.2 | 61.89±0.1 | 83.57±0.3 | 83.77±0.2 | 83.91±0.2 |

Table 1: Macro-F1 score comparisons on three dynamic graph datasets with different training ratios. The results are averaged over five runs, and the best results are in boldface. - denotes time-consuming.

| Methods | DBLP | | | Tmall | | | Patent | | |
|--------------------|------------------|------------------|------------------|------------------|------------------|------------------|------------------|------------------|------------------|
| | 40% | 60% | 80% | 40% | 60% | 80% | 40% | 60% | 80% |
| DeepWalk | 66.53 | 66.89 | 66.38 | 57.11 | 57.34 | 57.88 | 71.57±1.3 | 71.53±1.0 | 71.38±1.2 |
| Node2Vec | 66.80 | 67.37 | 67.31 | 60.41 | 60.56 | 60.66 | 69.01±0.9 | 69.08±0.9 | 68.99±1.0 |
| HTNE | 67.68 | 68.24 | 68.36 | 54.81 | 54.89 | 54.93 | - | - | - |
| M ² DNE | 69.23 | 69.47 | 69.71 | 64.21 | 64.38 | 64.65 | - | - | - |
| DyTriad | 65.13 | 66.80 | 66.95 | 53.24 | 56.88 | 60.72 | - | - | - |
| MPNN | 65.72±0.4 | 66.79±0.6 | 67.74±0.3 | 57.82±0.7 | 57.66±0.5 | 58.07±0.6 | - | - | - |
| JODIE | 68.44±0.6 | 68.51±0.8 | 68.80±0.9 | 58.36±0.5 | 60.28±0.3 | 60.49±0.3 | 77.64±0.7 | 77.89±0.5 | 77.93±0.4 |
| EvolveGCN | 69.12±0.8 | 70.43±0.6 | 71.32±0.5 | 59.96±0.7 | 61.19±0.6 | 61.77±0.6 | 79.39±0.5 | 79.75±0.3 | 80.01±0.3 |
| TGAT | 71.10±0.2 | 71.85±0.4 | 73.12±0.3 | 62.05±0.5 | 62.92±0.4 | 63.32±0.7 | 80.79±0.7 | 80.81±0.6 | 80.93±0.6 |
| SpikeNet | 71.98±0.3 | 72.35±0.8 | 74.86±0.5 | 63.52±0.7 | 64.84±0.4 | 66.10±0.3 | 83.48±0.8 | 83.80±0.7 | 83.88±0.9 |
| Dy-SIGN | 71.90±0.1 | 72.61±0.4 | 74.96±0.2 | 62.93±0.3 | 64.10±0.3 | 65.82±0.2 | 83.50±0.2 | 83.47±0.1 | 83.90±0.2 |

Table 2: Micro-F1 score comparisons on three dynamic graph datasets with different training ratios. The results are averaged over five runs, and the best results are in boldface. - denotes time-consuming.

lated as:

$$\hat{\mathbf{y}} = FC(\|\|_{t=1}^T \mathbf{a}^*), \mathcal{L} = - \sum_{r \in \mathbf{y}_L} \mathbf{y}_r \ln \hat{\mathbf{y}}_r, \quad (11)$$

where $\|\|$ denotes the concatenation operation, FC is the fully connect layer, $\hat{\mathbf{y}}$ is the nodes prediction, \mathbf{y} is the ground-truth labels, \mathbf{y}_L means the set of labeled nodes, and \mathcal{L} is the cross-entropy loss.

In summary, the proposed dynamic spiking graph neural network has several advantages. Firstly, \mathbf{a}_t^* is the fixed point of each time step on different layers, which can be considered as the hidden embeddings of time step t . Compared to traditional RNN-based dynamic graph methods, directly propagating \mathbf{a}_t^* over time would reduce the computational cost of calculating the hidden states and lower the model complexity. Secondly, traditional static feedback models usually set the initial states to 0, which cannot meet the requirement of dynamic graphs. By sending the previous state to the next time step, the model is able to capture the long temporal dependency for prediction. The detailed algorithm is shown in Algorithm 1.

Experiments

Experimental Settings

To verify the effectiveness of the proposed Dy-SIGN, we conduct experiments on three large real-world graph datasets, i.e., DBLP (Lu et al. 2019), Tmall (Lu et al. 2019) and Patent (Hall, Jaffe, and Trajtenberg 2001). The statistics and details introduction are presented in Appendix. We compared Dy-SIGN with various competing methods, including two static graph methods (i.e., DeepWalk (Perozzi, Al-Rfou, and Skiena 2014) and Node2Vec (Grover and Leskovec 2016)), seven dynamic graph methods (i.e., HTNE (Zuo et al. 2018), M²DNE (Lu et al. 2019), Dy-Triad (Zhou et al. 2018), MPNN (Panagopoulos, Nikolettos, and Vazirgiannis 2021), JODIE (Kumar, Zhang, and Leskovec 2019), EvolveGCN (Pareja et al. 2020) and TGAT (da Xu et al. 2020)), and one spiking method SpikeNet (Li et al. 2023). The details are introduced in Appendix. As for the implementation, we follow the same settings with (Li et al. 2023) and report the Macro-F1 and Micro-F1 results under different training ratios (i.e., 40%,

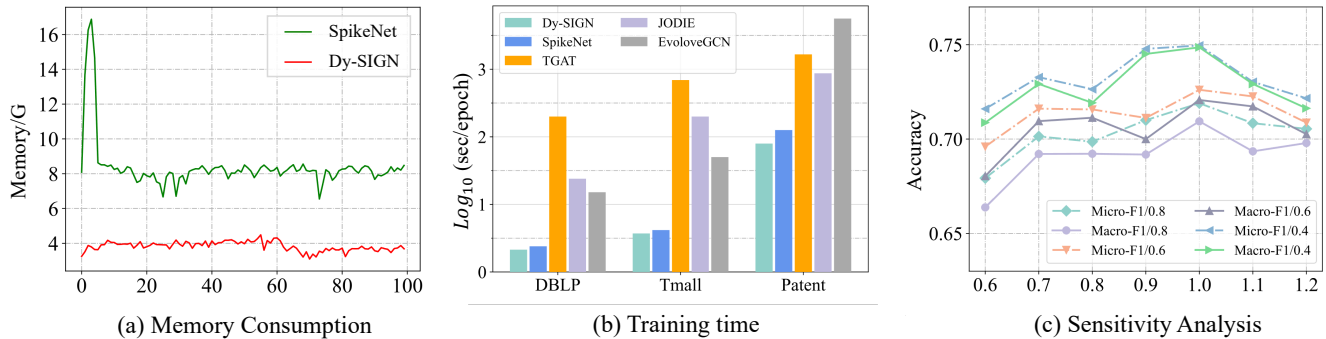


Figure 2: (a) The memory consumption of SpikeNet and Dy-SIGN on DBLP dataset. (b) The training time of different methods. (c) Hyperparameter sensitivity analysis of λ .

60%, and 80%). Besides, we use 5% for validation. The hidden dimension of all the methods is set to 128, and the batch size to 1024. The total training epochs are 100 and the learning rate is 0.001.

Performance Comparison

Comparison of Performance. The classification results on different datasets under various training ratios are presented in Table 1 and 2. From the results, we find that the proposed Dy-SIGN achieves competitive performance compared with other methods. From the results, we have the following observations: (1) The static methods DeepWalk and Node2Vec perform worse than the others, which indicates that simply applying static graph methods to dynamic graphs ignores the contribution of historical information for representation. (2) The methods HTNE, M²DNE, DyTrid, and MPNN fail to learn meaningful representations on the large-scale Patent dataset. The potential reason behind this is the high computational complexity of these models, leading to extensive time consumption for both training and prediction. This makes it impractical to achieve competitive performance within an acceptable time frame. (3) Although the spiking methods SpikeNet and Dy-SIGN apply the binary information for representation learning, the performance is still better than JODIE, EvolveGCN, and TGAT. This phenomenon indicates that the spike-based learning method is also competitive in both computational complexity and performance compared to the traditional methods. (4) The proposed Dy-SIGN outperforms SpikeNet in half of the settings. However, as shown in Figure 2 (a), the memory consumption of Dy-SIGN is about only half of SpikeNet under the same experiment environment, demonstrating the superiority of Dy-SIGN. We attribute this to the fact that by applying the variation training method, Dy-SIGN achieves more efficient results.

Comparison of Runtime Complexity. We further compare the runtime complexity between Dy-SIGN with SpikeNet, JODIE, EvolveGCN, and TGAT, which is shown in Figure 2 (b). From the results, we find that the SNN-based methods are significantly more efficient than the ANNs methods. The reason for this is attributed to the fact that

SNN-based methods use binary signals instead of continuous features, allowing the matrix multiplication operation to be replaced by an accumulation operation. Additionally, the proposed Dy-SIGN is slightly more efficient than SpikeNet method, the potential reason is that Dy-SIGN uses the simple form to calculate the gradient with Equation 8, ignoring the time-consuming calculation of gradient in BPTT.

Sensitivity Analysis

In this section, we examine the impact of hyperparameters on the performance of our proposed Dy-SIGN. Specifically, the parameter λ determines the amount of information retained for the next time latency step representation. We test the values of λ in the range of $\{0.6, 0.7, 0.8, 0.9, 1, 1.1, 1.2\}$ with other parameters fixed to determine the optimal value. The results are depicted in Figure 2 (c). From the results, we observe that as the value of λ increases, the performance initially improves and then gradually declines. We attribute the reason to the fact that the smaller λ cannot provide sufficient historical information for effective representation learning. On the other hand, larger λ may lead to worse performance since the current time latency step representation may be influenced by too much historical information. Thus, we set the default value of λ to 1.

Conclusion

In this paper, we study the problem of combining SNNs with dynamic graphs using implicit differentiation for node classification and propose a novel method named Dy-SIGN. To tackle the issue of information loss on graph structure and details during SNN propagation, we propose an information compensation mechanism. This mechanism passes the original structure and features to the last layer of the network, which then participates in node representation learning. This structure is very similar to traditional feedback models. Based on this, we use explicit differentiation and a variation training method to address the issue of high memory consumption in the combination of SNNs and dynamic graphs. Extensive experiments on real-world large-scale datasets validate the superiority of the proposed Dy-SIGN.

Acknowledgments

This work is part of the research project “ENERGY-BASED PROBING FOR SPIKING NEURAL NETWORKS”, performed at Mohamed bin Zayed University of Artificial Intelligence (MBZUAI), funded by Technology Innovation Institute (TII) (Contract No. TII/ARRC/2073/2021).

References

- Bai, S.; Kolter, J. Z.; and Koltun, V. 2019. Deep equilibrium models. In *NeurIPS*.
- Bai, S.; Koltun, V.; and Kolter, J. Z. 2020. Multiscale deep equilibrium models. In *NeurIPS*.
- Bellec, G.; Salaj, D.; Subramoney, A.; Legenstein, R.; and Maass, W. 2018. Long short-term memory and learning-to-learn in networks of spiking neurons. In *NeurIPS*, volume 31.
- Bohte, S.; Kok, J.; and La Poutre, H. 2000. SpikeProp: Backpropagation for Networks of Spiking Neurons Error-Backpropagation in a Network of Spiking Neurons. In *ESANN*.
- Brette, R.; Rudolph, M.; Carnevale, T.; Hines, M.; Beeman, D.; Bower, J. M.; Diesmann, M.; Morrison, A.; Goodman, P. H.; Harris, F. C.; et al. 2007. Simulation of networks of spiking neurons: a review of tools and strategies. *Journal of computational neuroscience*, 23: 349–398.
- Bu, T.; Ding, J.; Yu, Z.; and Huang, T. 2022. Optimized potential initialization for low-latency spiking neural networks. In *AAAI*.
- Chen, S.; Li, Z.; and Tang, Z. 2020. Relation R-CNN: A Graph Based Relation-Aware Network for Object Detection. *IEEE Signal Processing Letters*, 27.
- Cho, K.; Van Merriënboer, B.; Gulcehre, C.; Bahdanau, D.; Bougares, F.; Schwenk, H.; and Bengio, Y. 2014. Learning phrase representations using RNN encoder-decoder for statistical machine translation. *arXiv preprint arXiv:1406.1078*.
- Chung, F.; and Lu, L. 2002. Connected components in random graphs with given expected degree sequences. *Annals of combinatorics*, 6(2): 125–145.
- da Xu; chuanwei ruan; evren korpeoglu; sushant kumar; and kannan achan. 2020. Inductive representation learning on temporal graphs. In *ICLR*.
- Diehl, P. U.; Neil, D.; Binas, J.; Cook, M.; Liu, S.-C.; and Pfeiffer, M. 2015. Fast-classifying, high-accuracy spiking deep networks through weight and threshold balancing. In *IJCNN*.
- Esser, S. K.; Appuswamy, R.; Merolla, P.; Arthur, J. V.; and Modha, D. S. 2015. Backpropagation for energy-efficient neuromorphic computing. In *NeurIPS*, volume 28.
- Fey, M.; and Lenssen, J. E. 2019. Fast graph representation learning with PyTorch Geometric. *arXiv preprint arXiv:1903.02428*.
- Grover, A.; and Leskovec, J. 2016. node2vec: Scalable feature learning for networks. In *KDD*.
- Gu, F.; Chang, H.; Zhu, W.; Sojoudi, S.; and El Ghaoui, L. 2020. Implicit graph neural networks. *NeurIPS*.
- Hall, B. H.; Jaffe, A. B.; and Trajtenberg, M. 2001. The NBER patent citation data file: Lessons, insights and methodological tools.
- Hochreiter, S. 1998. The vanishing gradient problem during learning recurrent neural nets and problem solutions. *International Journal of Uncertainty, Fuzziness and Knowledge-Based Systems*, 6(02): 107–116.
- Hochreiter, S.; and Schmidhuber, J. 1997. Long short-term memory. *Neural computation*, 9(8): 1735–1780.
- Huh, D.; and Sejnowski, T. J. 2018. Gradient descent for spiking neural networks. In *NeurIPS*.
- Hunsberger, E.; and Eliasmith, C. 2015. Spiking deep networks with LIF neurons. *arXiv preprint arXiv:1510.08829*.
- Ju, W.; Yi, S.; Wang, Y.; Xiao, Z.; Mao, Z.; Li, H.; Gu, Y.; Qin, Y.; Yin, N.; Wang, S.; et al. 2024. A survey of graph neural networks in real world: Imbalance, noise, privacy and ood challenges. *arXiv preprint arXiv:2403.04468*.
- Kim, S.; Park, S.; Na, B.; and Yoon, S. 2020. Spiking-YOLO: spiking neural network for energy-efficient object detection. In *AAAI*.
- Kumar, S.; Zhang, X.; and Leskovec, J. 2019. Predicting dynamic embedding trajectory in temporal interaction networks. In *KDD*.
- Li, J.; Yu, Z.; Zhu, Z.; Chen, L.; Yu, Q.; Zheng, Z.; Tian, S.; Wu, R.; and Meng, C. 2023. Scaling Up Dynamic Graph Representation Learning via Spiking Neural Networks. In *AAAI*.
- Liu, J.; Hooi, B.; Kawaguchi, K.; and Xiao, X. 2022. MGNNI: Multiscale Graph Neural Networks with Implicit Layers. In *NeurIPS*.
- Lu, Y.; Wang, X.; Shi, C.; Yu, P. S.; and Ye, Y. 2019. Temporal network embedding with micro-and macro-dynamics. In *CIKM*.
- Maass, W. 1997. Networks of spiking neurons: the third generation of neural network models. *Neural networks*, 10(9): 1659–1671.
- Meng, Q.; Xiao, M.; Yan, S.; Wang, Y.; Lin, Z.; and Luo, Z.-Q. 2022. Training high-performance low-latency spiking neural networks by differentiation on spike representation. In *CVPR*.
- Mi, L.; and Chen, Z. 2020. Hierarchical graph attention network for visual relationship detection. In *CVPR*.
- Panagopoulos, G.; Nikolentzos, G.; and Vazirgiannis, M. 2021. Transfer graph neural networks for pandemic forecasting. In *AAAI*.
- Pang, J.; Wang, Z.; Tang, J.; Xiao, M.; and Yin, N. 2023. Sgda: Spectral augmentation for graph domain adaptation. In *Proceedings of the 31st ACM international conference on multimedia*, 309–318.
- Pareja, A.; Domeniconi, G.; Chen, J.; Ma, T.; Suzumura, T.; Kanezashi, H.; Kaler, T.; Schardl, T.; and Leiserson, C. 2020. Evolvegn: Evolving graph convolutional networks for dynamic graphs. In *AAAI*.
- Paszke, A.; Gross, S.; Chintala, S.; Chanan, G.; Yang, E.; DeVito, Z.; Lin, Z.; Desmaison, A.; Antiga, L.; and Lerer, A. 2017. Automatic differentiation in pytorch.

- Perozzi, B.; Al-Rfou, R.; and Skiena, S. 2014. Deepwalk: Online learning of social representations. In *KDD*, 701–710.
- Pfeiffer, M.; and Pfeil, T. 2018. Deep learning with spiking neurons: Opportunities and challenges. *Frontiers in neuroscience*, 12: 774.
- Rathi, N.; Srinivasan, G.; Panda, P.; and Roy, K. 2020. Enabling Deep Spiking Neural Networks with Hybrid Conversion and Spike Timing Dependent Backpropagation. In *ICML*.
- Rossi, E.; Chamberlain, B.; Frasca, F.; Eynard, D.; Monti, F.; and Bronstein, M. 2020. Temporal graph networks for deep learning on dynamic graphs. *arXiv preprint arXiv:2006.10637*.
- Rueckauer, B.; Lungu, I.-A.; Hu, Y.; Pfeiffer, M.; and Liu, S.-C. 2017. Conversion of continuous-valued deep networks to efficient event-driven networks for image classification. *Frontiers in neuroscience*, 11: 682.
- Sak, H.; Senior, A.; and Beaufays, F. 2014. Long short-term memory based recurrent neural network architectures for large vocabulary speech recognition. *arXiv preprint arXiv:1402.1128*.
- Scarselli, F.; Gori, M.; Tsoi, A. C.; Hagenbuchner, M.; and Monfardini, G. 2008. The graph neural network model. *IEEE Transactions on Neural Networks*, 20(1): 61–80.
- Schlichtkrull, M.; Kipf, T. N.; Bloem, P.; Van Den Berg, R.; Titov, I.; and Welling, M. 2018. Modeling relational data with graph convolutional networks. In *European Semantic Web Conference*.
- Schliebs, S.; and Kasabov, N. 2013. Evolving spiking neural network—a survey. *Evolving Systems*, 4: 87–98.
- Shi, M.; Huang, Y.; Zhu, X.; Tang, Y.; Zhuang, Y.; and Liu, J. 2021. GAEN: graph attention evolving networks. In *IJCAI*.
- Shrestha, S. B.; and Orchard, G. 2018. Slayer: Spike layer error reassignment in time. In *NeurIPS*.
- Thiele, J. C.; Bichler, O.; and Dupret, A. 2020. SpikeGrad: An ANN-equivalent Computation Model for Implementing Backpropagation with Spikes. In *ICML*.
- Wieder, O.; Kohlbacher, S.; Kuenemann, M.; Garon, A.; Ducrot, P.; Seidel, T.; and Langer, T. 2020. A compact review of molecular property prediction with graph neural networks. *Drug Discovery Today: Technologies*, 37: 1–12.
- Wu, H.; Zhang, Y.; Weng, W.; Zhang, Y.; Xiong, Z.; Zha, Z.-J.; Sun, X.; and Wu, F. 2021. Training spiking neural networks with accumulated spiking flow. In *AAAI*.
- Wu, S.; Sun, F.; Zhang, W.; Xie, X.; and Cui, B. 2022. Graph neural networks in recommender systems: a survey. *ACM Computing Surveys*, 55(5): 1–37.
- Xiao, M.; Meng, Q.; Zhang, Z.; He, D.; and Lin, Z. 2022. Online Training Through Time for Spiking Neural Networks. In *NeurIPS*.
- Xiao, M.; Meng, Q.; Zhang, Z.; Wang, Y.; and Lin, Z. 2021. Training feedback spiking neural networks by implicit differentiation on the equilibrium state. In *NeurIPS*.
- Xu, D.; Cheng, W.; Luo, D.; Liu, X.; and Zhang, X. 2019a. Spatio-Temporal Attentive RNN for Node Classification in Temporal Attributed Graphs. In *IJCAI*.
- Xu, H.; Jiang, C.; Liang, X.; and Li, Z. 2019b. Spatial-aware graph relation network for large-scale object detection. In *CVPR*.
- Xu, M.; Wu, Y.; Deng, L.; Liu, F.; Li, G.; and Pei, J. 2021. Exploiting spiking dynamics with spatial-temporal feature normalization in graph learning. In *IJCAI*.
- Yin, N.; Feng, F.; Luo, Z.; Zhang, X.; Wang, W.; Luo, X.; Chen, C.; and Hua, X.-S. 2022a. Dynamic hypergraph convolutional network. In *ICDE*.
- Yin, N.; Shen, L.; Li, B.; Wang, M.; Luo, X.; Chen, C.; Luo, Z.; and Hua, X.-S. 2022b. DEAL: An Unsupervised Domain Adaptive Framework for Graph-level Classification. In *Proceedings of the 30th ACM International Conference on Multimedia*, 3470–3479.
- Yin, N.; Shen, L.; Wang, M.; Lan, L.; Ma, Z.; Chen, C.; Hua, X.-S.; and Luo, X. 2023a. CoCo: A Coupled Contrastive Framework for Unsupervised Domain Adaptive Graph Classification. *arXiv preprint arXiv:2306.04979*.
- Yin, N.; Shen, L.; Xiong, H.; Gu, B.; Chen, C.; Hua, X.-S.; Liu, S.; and Luo, X. 2023b. Messages are never propagated alone: Collaborative hypergraph neural network for time-series forecasting. *IEEE Transactions on Pattern Analysis & Machine Intelligence*, (01): 1–15.
- Yin, N.; Wan, M.; Shen, L.; Patel, H. L.; Li, B.; Gu, B.; and Xiong, H. 2024a. Continuous Spiking Graph Neural Networks. *arXiv preprint arXiv:2404.01897*.
- Yin, N.; Wang, M.; Chen, Z.; Shen, L.; Xiong, H.; Gu, B.; and Luo, X. 2024b. DREAM: Dual structured exploration with mixup for open-set graph domain adaptation. In *The Twelfth International Conference on Learning Representations*.
- Zhou, L.; Yang, Y.; Ren, X.; Wu, F.; and Zhuang, Y. 2018. Dynamic network embedding by modeling triadic closure process. In *AAAI*.
- Zhou, S.; Li, X.; Chen, Y.; Chandrasekaran, S. T.; and Sanyal, A. 2021. Temporal-coded deep spiking neural network with easy training and robust performance. In *AAAI*.
- Zhu, Z.; Peng, J.; Li, J.; Chen, L.; Yu, Q.; and Luo, S. 2022. Spiking Graph Convolutional Networks. In *IJCAI*.
- Zuo, Y.; Liu, G.; Lin, H.; Guo, J.; Hu, X.; and Wu, J. 2018. Embedding temporal network via neighborhood formation. In *KDD*.

Table 3: The specific statistics of the experimental datasets.

| Dataset | #Nodes | #Edges | #Classes | #Time steps |
|---------|-----------|------------|----------|-------------|
| DBLP | 28,085 | 236,894 | 10 | 27 |
| Tmall | 577,314 | 4,807,545 | 5 | 186 |
| Patent | 2,738,012 | 13,960,811 | 6 | 25 |

Datasets

In our work, we conduct our experiments on three public large-scale graph datasets, i.e., DBLP (Lu et al. 2019), Tmall (Lu et al. 2019) and Patent (Hall, Jaffe, and Trajtenberg 2001). The statistics of the datasets are presented in Table 3, and the details introduction are as follows:

- **DBLP.** DBLP (Lu et al. 2019) is an academic co-author graph that is derived from the extensive bibliography website. This dataset is widely used in research to study various aspects of academic collaborations and knowledge dissemination within the scientific community. In the DBLP graph, each node represents an author, while edges between nodes indicate collaborative relationships between pairs of authors who have jointly published papers together.
- **Tmall.** Tmall (Lu et al. 2019) is a bipartite graph that is constructed from sales data gathered in 2014 from the popular e-commerce platform Tmall.com. This dataset captures the interactions between users and items, where each node represents either a user or an item, and each edge corresponds to a purchase transaction along with a timestamp indicating the time of the purchase. In the Tmall dataset, users are connected to items based on their purchasing behavior. This rich interaction data provides valuable insights into user preferences, item popularity, and the dynamics of e-commerce transactions. The dataset is particularly interesting for studying recommendation systems, personalized marketing, and understanding user-item interactions in an online retail environment.
- **Patent.** The Patent dataset (Hall, Jaffe, and Trajtenberg 2001) is a citation network consisting of United States patents spanning the years 1963 to 1999. This dataset provides a valuable resource for studying the interconnections and relationships between patents in various domains. Each node in the Patent dataset represents a patent, and the edges between the nodes indicate citation relationships, where one patent cites another. This citation network captures the flow of knowledge and innovation within the patent system. The dataset contains patents from diverse technological domains and covers a wide range of topics and industries.

Baselines

In this section, we compared the proposed Dy-SIGN with a wide range of competing approaches, the details introduction is as follows:

Static Graph Methods. We compare the proposed Dy-SIGN with two widely used static graph methods,

i.e., DeepWalk (Perozzi, Al-Rfou, and Skiena 2014) and Node2Vec (Grover and Leskovec 2016). For these baselines, we set the drop rate in the range of $\{0.1, 0.3, 0.5, 0.7\}$ to select the best performance, the embedding size of all methods is set to 128 as default for the sake of fairness.

- **DeepWalk.** DeepWalk (Perozzi, Al-Rfou, and Skiena 2014) performs random walks to generate an ordered sequence of nodes from a static graph to create contexts for each node, then applies a skip-gram model to these sequences to learn representations. DeepWalk (Perozzi, Al-Rfou, and Skiena 2014) is a graph embedding method that leverages random walks to capture the structural information of a static graph. The main idea behind DeepWalk is to generate sequences of nodes by performing random walks on the graph and then learn node representations from these sequences.
- **Node2Vec.** Node2Vec (Grover and Leskovec 2016) is an extension of the DeepWalk algorithm that incorporates biased random walks to explore the neighborhood of nodes and learn representations on a static graph. Node2Vec has been widely used for various graph analysis tasks, such as node classification, link prediction, and visualization. By incorporating biased random walks, Node2Vec can capture both the local and global structural characteristics of a graph, providing more informative and expressive node embeddings.

Dynamic Graph Methods. We also compare the proposed Dy-SIGN with eight dynamic graph methods, i.e., HTNE (Zuo et al. 2018), M²DNE (Lu et al. 2019), Dy-Triad (Zhou et al. 2018), MPNN (Panagopoulos, Nikolettos, and Vazirgiannis 2021), JODIE (Kumar, Zhang, and Leskovec 2019), EvolveGCN (Pareja et al. 2020), TGAT (da Xu et al. 2020) and SpikeNet (Li et al. 2023). We implement all the models with the codes provided by the corresponding paper. We search the hyperparameters by ranging the learning rate over $\{0.01, 0.005, 0.001, 0.0005, 0.0001\}$ and dropout rate over $\{0.3, 0.5, 0.7\}$ and report the best reports. For fairness, we set the embedding size of all the models to 128 as default.

- **HTNE.** HTNE (Zuo et al. 2018) is a network embedding method that combines the Hawkes process and attention mechanism to capture the formation sequences of neighborhoods in a network. By integrating the Hawkes process and attention mechanism, HTNE can effectively capture the temporal dynamics and interaction patterns in network neighborhoods. This enables the learned embeddings to better represent the evolving nature of network structures and facilitate various downstream tasks such as link prediction, community detection, and anomaly detection.
- **M²DNE.** M²DNE (Lu et al. 2019) is a network embedding method that specifically focuses on capturing the structural and temporal properties of evolving graphs. It achieves this by incorporating a temporal attention point process and a general dynamics equation into the embedding process.
- **DyTriad.** DyTriad (Zhou et al. 2018) is a dynamic network modeling approach that combines the modeling of

structural information and evolution patterns based on the triadic closure process. By incorporating both aspects, Dy-Triad is able to effectively capture the dynamics of evolving graphs.

- **MPNN.** MPNN (Panagopoulos, Nikolentzos, and Vazirgiannis 2021) is a time-series variant of the message-passing neural network (MPNN) that incorporates a two-layer LSTM (Long Short-Term Memory). MPNN is designed to capture long-range temporal dependencies in temporal graphs by encoding the dynamics into the node representations.
- **JODIE.** JODIE (Kumar, Zhang, and Leskovec 2019) utilizes a dual Recurrent Neural Network (RNN) architecture to update node embeddings in an evolving graph based on observed interactions. This approach enables the prediction of future embedding trajectories.
- **EvolveGCN.** EvolveGCN (Pareja et al. 2020) is a method that incorporates Recurrent Neural Networks (RNNs) to dynamically evolve the parameters of Graph Neural Networks (GNNs) over time. By adapting the GNN parameters at each time step, EvolveGCN effectively captures the evolving dynamics of a sequence of graphs.
- **TGAT.** TGAT (da Xu et al. 2020) is an inductive learning method specifically designed for dynamic graph data. It leverages self-attention mechanisms as fundamental building blocks and introduces a functional time encoding scheme to effectively capture both temporal and topological information in dynamic graphs. This approach has demonstrated state-of-the-art performance across various dynamic graph learning tasks.
- **SpikeNet.** SpikeNet (Li et al. 2023) introduces a scalable framework designed to effectively capture both the temporal dynamics and structural patterns of temporal graphs. This framework addresses the challenge of efficiently analyzing large-scale temporal graph data.

Our Method

We implement the proposed Dy-SIGN with PyTorch (Paszke et al. 2017) and PyTorch Geometric library (Fey and Lenssen 2019). For the implementation, we adopt the identical settings as described in (Li et al. 2023) and present the evaluation results in terms of Macro-F1 and Micro-F1 scores using various training ratios, namely 40%, 60%, and 80%. Additionally, we allocate 5% of the data for validation purposes. In our implementation, we set the hidden dimension of all methods to 128 to ensure consistency. The batch size is configured as 1024 to balance computational efficiency and model performance. To train the models effectively, we conduct a total of 100 training epochs and employ a learning rate of 0.001. These settings allow for a fair and consistent evaluation across different methods, enabling us to assess their performance under comparable conditions. By reporting Macro-F1 and Micro-F1 scores, we can comprehensively evaluate the models' performance in terms of both overall and individual class classification accuracy. Overall, our implementation follows a standardized approach, ensuring reproducibility and facilitating meaningful comparisons between different methods.